AEROSPACE REPORT NO.
TOR-2019-02016

REACH Dosimeter Equivalent Energy Thresholds and Flux Conversion Factors

July 1, 2019

T. Paul O'Brien[1], Mark D. Looper[1], and Joseph E. Mazur[2]
[1]Space Sciences Department, Space Science Applications Laboratory
[2]Space Science Applications Laboratory, Physical Sciences Laboratories

Prepared for:

Space and Missile Systems Center
Air Force Space Command
483 N. Aviation Blvd.
El Segundo, CA 90245-2808

Contract No. FA8802-19-C-0001

Authorized by: Space Systems Group

Acknowledgments

The authors acknowledge W. Crain for help confirming the characteristics of the dosimeters,
S. Claudepierre for developing some of the spectral shapes chosen for the bowtie analysis, and J.B. Blake for performing essential laboratory calibrations of the dosimeters.

Abstract

In this report, we provide coefficients that can be used to convert counts per second and dose rate from the dosimeters in the Responsive Environmental Assessment Commercially Hosted (REACH) program in low Earth orbit into particle fluxes in equivalent integral energy channels. We provide these factors for users wishing to interpret the REACH sensor data as isotropic particle number flux, in integral energy channels, for electrons or protons. One set of REACH sensors uses energy deposit thresholds to discriminate between protons and electrons. Other sensors require inference based on sensor location or by combining multiple sensors together. We derived conversion factors from a bowtie analysis of Geant4 simulations of the REACH dosimeter response [2][3][4]. In the bowtie analysis, multiple probable approximate candidate particle spectra are used to relate the expected count rate, flux conversion factor, and energy threshold for an idealized integral energy channel. Then the energy threshold and flux conversion factor are chosen to minimize the error in the estimated flux across those probable spectra. In our analysis, we use power law and exponential spectral shapes that have been observed in space by scientific spectrometers on other missions. For the dosimeter with the lowest-energy threshold, we introduce a power-law tail to counteract the unphysical effects of extrapolating very flat candidate spectral shapes that are reasonable near that low-energy threshold to much higher energies that penetrate the shielding off-axis.

Executive Summary

We have performed a bowtie analysis to obtain proton and electron equivalent energy thresholds and flux conversion factors for the six dosimeter varieties (flavors) carried on the REACH pods in low Earth orbit. These results consolidate the full 3-D response obtained from a Geant4 simulation into scaling factors suitable for routine conversion from sensor count rates and dose rates to particle number flux.

The bowtie analysis produces an energy threshold E_0 and a flux conversion factor G, such that the isotropic integral number flux above E_0 can be estimated from the dosimeter count rate r according to:

$$j_>(E_0) = \frac{r}{G}$$

with units #/cm^2/sr/s. It is also sometimes useful to compute an omnidirectional number flux $J_>(E_0)$ with units #/cm^2/s, and this would be:

$$J_>(E_0) = 4\pi j_>(E_0) = \frac{4\pi r}{G}$$

The values in Table 1 can be used to evaluate either of these equations to obtain estimates of the proton or electron omnidirectional integral number flux from individual REACH dosimeter dose count rates. We also provide G^*, which allows for conversion of dose rates into integral particle flux.

Table 1. Bowtie Results for REACH Dosimeters

Flavor	Electrons				Protons			
	E_0 (MeV)	$G^{(2)}$ (cm^{2}sr)	$G^{*(3)}$ (cm^{2}sr rad)	G error$^{(4)}$ (%)	E_0 (MeV)	$G^{(2)}$ (cm^{2}sr)	$G^{*(3)}$ (cm^{2}sr rad)	G error$^{(4)}$ (%)
U$^{(1)}$	2.15	4.3E-5	6.7E-10	110	51.5	4.0E-2	6.2E-7	1
V$^{(1)}$	2.20	5.9E-5	9.2E-10	103	43.9	3.6E-2	5.6E-7	2
W	1.43	4.5E-6	9.3E-11	7	10.5	1.1E-2	2.2E-7	<1
X	0.798	9.1E-4	1.4E-8	7	12.1	2.1E-2	3.3E-7	4
Y$^{(1)}$	2.47	1.6E-4	2.5E-9	77	30.3	2.9E-2	4.6E-7	4
Z	0.0916	2.6E-6	7.3E-10	20	1.29	3.3E-5	9.4E-9	9

(1) The approximation to an ideal integral electron channel has large uncertainties for these channels due to the absence of a sharp turn-on in the response function.
(2) Factor for converting dosimeter counts per second to flux.
(3) Factor for converting dosimeter rads per second to flux.
(4) Conversion factor errors are percentages that apply to both G and G^*

Regardless of whether the source of the particle data is a dosimeter or a more sophisticated spectrometer, fluxes computed from bowtie analyses should not be used in 3-D data assimilation or spectral inversion. Data assimilation and spectral inversion require the detailed sensor response. To that end, we have archived the simulated 3-D (incident energy, angle, angle) response for all six dosimeter flavors.

Contents

Figures

Tables

1. Introduction

The Responsive Environmental Assessment Commercially Hosted (REACH) program consists of 32 sensor pods in 800 km polar orbit. Each pod carries two dosimeters designed by The Aerospace Corporation and manufactured by Teledyne Microelectronics, Inc. The pods come in four options, denoted model 0 through 3, combining different combinations of energy threshold and shielding to yield six dosimeter varieties (denoted flavor U through Z). Table 2 shows which dosimeter flavors are carried on which REACH pod models and which hosted payload numbers (HPLs) carry each pod model. We note that in this document, we refer to the dosimeters within a pod as Dos1 and Dos2, but elsewhere they are referred to as DosA and DosB, respectively.

Table 2. Dosimeter Flavors by REACH Pod Model and Payload Numbers

Model	Dos1	Dose2	HPL Numbers
0	X	Z	169, 170, 171, 172, 181, 180
1	X	W	101, 115, 114, 133, 137, 135, 136, 108, 139, 162, 176, 164, 149, 173
2	Y	V	116, 102, 113, 140, 148, 163, 166
3	Y	U	105, 134, 138, 165, 175

From a detector perspective, there are three dosimeter variants: a LowLET or NuDos dosimeter, a MedLET or standard dosimeter, and a HiLET dosimeter. The LowLET silicon detector is 1.8 mm in diameter, 60 μm thick, and requires an energy deposit of at least 30 keV to register a sensor count. The MedLET and HiLET dosimeters are rectangular, 3 × 7 mm across, and 250 μm thick. The MedLET dosimeter requires a deposit of at least 100 keV to register a count, and the HiLET dosimeter requires a deposit of at least 1 MeV to register a count. The six flavors are obtained by further varying the amount of added Mallory shielding over the top of the MedLET dosimeters. The MedLET dosimeters have been used to measure dose in lunar and Earth orbit [5][6][7], and all three variants were flown on the AeroCube-6 mission in preparation for REACH [8].

To determine the conversion from dosimeter count to energy deposit, we rely on calibrations performed with a ^{148}Gd radiation source, which produces 3.183 MeV α particles according to the following decay reaction:

$$^{148}\mathrm{Gd} \rightarrow {}^{144}\mathrm{Sm} + \alpha (3.183\ \mathrm{MeV})$$

By measuring the count rate in each dosimeter variant, we can determine how much energy it takes to produce a count. Using the detector mass, we can then determine the dose associated with each count. We note that the values obtained by this procedure differ slightly from those used on AeroCube-6. The dosimeters output accumulator values rather than count rates, so operationally one must numerically differentiate the accumulated counts to obtain the count rate. A dose-per-count value is then used to convert from accumulator counts to dose and from count rate to dose rate.

Table 3 provides a summary of the physical and electronic properties of the dosimeters. Figure 1 provides a photograph of a REACH pod and its two dosimeters enclosed in their Mallory shields, as well as the coordinate system used in the simulation and archived response files.

We note that this report has much in common with the AeroCube-6 dosimeter bowtie analysis report [9]. A report on ground calibration and comparison of REACH space-based observations to other space-based observations will be presented in a future instrument paper.

Table 3. Summary of Dosimeter Flavor Physical and Electronic Properties

Flavor	Added mils Mallory	Equivalent mils Al	Dosimeter Variant	Electronic Threshold keV	Energy/Count MeV	Dose/Count, µrads
Z	0	0	LowLET	30	6.27	282
Y	23	176	MedLET	100	11.9	15.6
X	0	32	MedLET	100	11.9	15.6
W	0	32	HiLET	1000	15.8	20.7
V	56	383	MedLET	100	11.9	15.6
U	80	533	MedLET	100	11.9	15.6

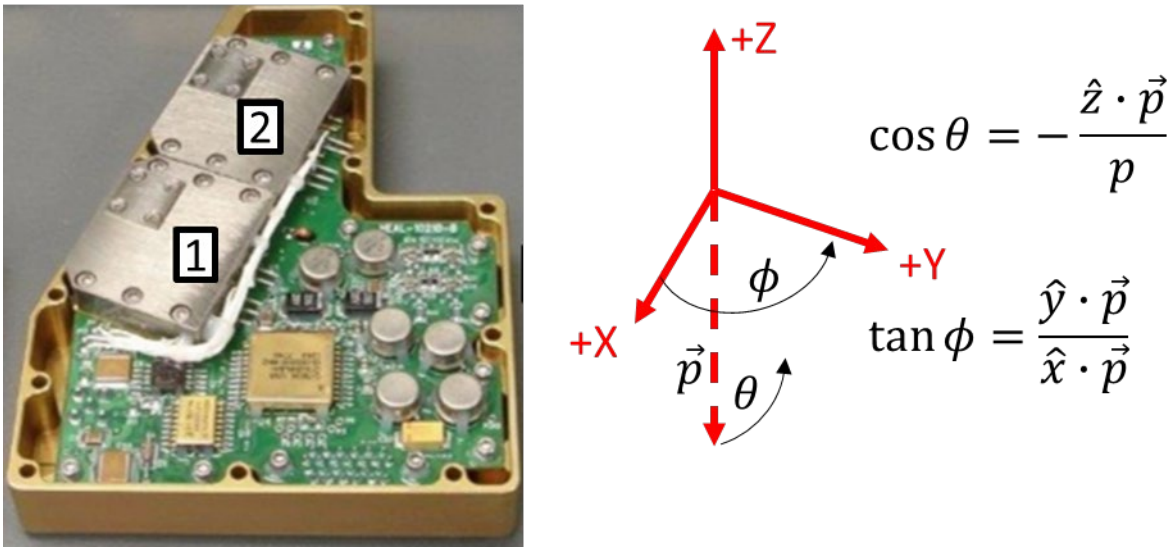

Figure 1. Photograph of a REACH pod with Dos1 and Dos2 labeled. Coordinate axes are also provided, as well as the relationship between incident particle momentum *p* and the coordinates.

2. Method

References [2], [3], and [4] describe a series of full-physics Geant4 simulations of the six REACH dosimeter flavors. In a forward Geant4 simulation, many test particles are simulated, each with unique incident energy, direction, and point of origin on the simulation boundary. Any energy deposited by the test particle in one of the Dos1 or Dos2 detectors is recorded for later tabulation. In a reverse or adjoint Geant4 simulation, a combination of backward and forward tracings is used to produce the same type of information, but with a weighting indicating that each test particle trajectory is more or less probable. These weighting factors are a side effect of computation optimization in the reverse method. The REACH dosimeter simulations use both methods to produce 3-D (energy, angle, angle) response functions. These functions are stored by pod model type and collected for all six flavors in files following the draft standard response file format maintained by the International Radiation Belt Environment Model Library (IRBEM-LIB). These standard files are built to aid in sophisticated inversions of the sensor response, such as spectral or angular inversions or global data assimilation. However, for most uses, it is desirable to have simpler energy thresholds and flux conversion factors so that each dose channel can be converted directly to proton or electron flux (based on context). To this end, we perform the bowtie analysis.

The following treatment is based in part on Appendix A of [7]. For a given dosimeter flavor, we start by integrating the simulated sensor response over all angles of incidence, which is equivalent to assuming that the incident flux is isotropic. This results in the response function, $R(E)$, which has units of cm^{2}sr and depends on incident particle energy E. Next, we consider the dose count rate we would expect if we knew the incident (isotropic) unidirectional differential flux $j(E)$. That dose count rate, r, is given by:

$$r = \int_0^\infty j(E)R(E)dE \approx G \int_{E_0}^\infty j(E)dE = G\, j_>(E_0)$$

where E_0 is the desired energy threshold, G is the flux conversion factor (effectively a geometric factor) with units cm^{2}sr, and $j_>(E_0)$ is the isotropic integral flux above energy E_0 having units of #/cm^2/sr/s. For any trial spectrum, we can obtain the flux conversion factor G as a function of the energy threshold E_0 for a corresponding ideal integral channel as:

$$G = \frac{r}{j_>(E_0)}$$

We repeat this process for many trial spectra and select the E_0 that produces the least squared error in the logarithm of G over the set of spectra. This approach minimizes the *relative* error in the flux conversion across the chosen variety of spectra. As we will see in the next section, the plot of the G versus E_0 relationships has some resemblance to a sartorial bowtie, and the best joint value of E_0 and G represents the knot in the bowtie.

3. Bowtie Results

We use two main families of spectral functions: power laws $j(E) = E^{-n}$ and exponentials $j(E) = \exp(-E/T)$. Using plots of $R(E)$, we can obtain an initial sense of what the energy threshold is for a given dosimeter and use that to examine spectra obtained by more sophisticated sensors to determine appropriate *typical* values of n and T. For the analysis of the flavor Z dosimeter, we also impose an E^{-5} power law tail for E>1 MeV electrons because we determined that the flatter spectra common near its ~100 keV threshold are not appropriately extrapolated to the >1 MeV regime.

Based on our experience with similar dosimeters on the Deal payload [7] and detailed measurements from sensors on the Van Allen Probes [10], we have selected the spectral parameters given in Table 4. These spectra represent typical conditions observed in the radiation belts, although nature provides an abundance of variety beyond these simple spectra.

Table 4. Spectra Assumed for Bowtie Analysis

Flavors	Electrons	Protons
Z	n~0.5,1,…4 T~20,40,…100 keV Tail: E^{-5} for E>1 MeV	n~4.6 (only one) T~100,200,300,400 keV
U,V,W,X,Y	n~2,3,…8 T~0.2,0.4,0.8,1.6,3.2 MeV	n~2,2.5,…4 T~None

Figures 2–4 show the bowtie analysis for individual channels. Each figure depicts the response function $R(E)$, the $G(E_0)$ curves for individual spectra, and the adopted E_0,G fit values from the bowtie analysis.

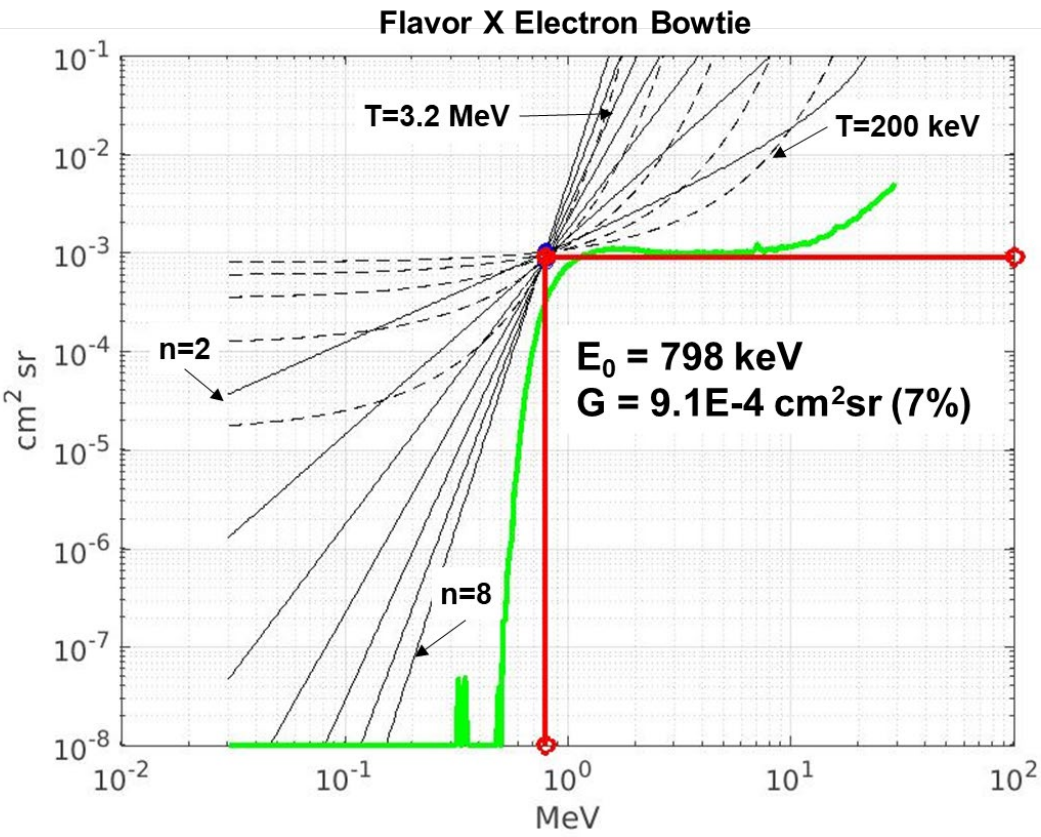

Figure 2. Bowtie analysis for the electron response of dosimeter flavor X. The simulated response function *R(E)* is in green. The solid black curves are $G(E_0)$ for power law spectra. The dashed black curves are $G(E_0)$ for exponential spectra. The blue circles (mostly hidden under the red dot) indicate the values of $G(E_0)$ for the different spectra at the best-fit E_0. Red indicates the adopted bowtie values of E_0 and G.

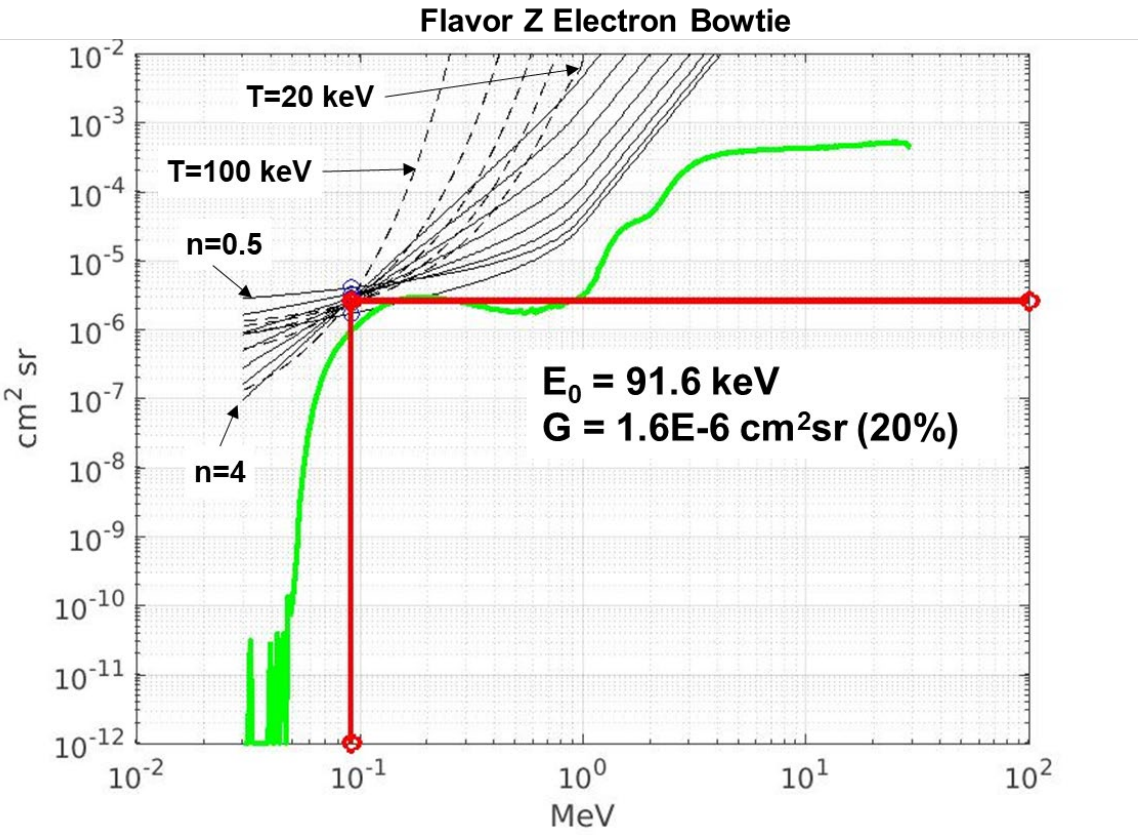

Figure 3. Bowtie analysis for the electron response of flavor X, in the same format as Figure 2. Note the presence of a second, stronger response at >1 MeV. The use of a >1 MeV power-law tail E^{-5} suppresses the influence of this penetrating response, based on the observation that, for electrons, flat spectra in the vicinity of ~100 keV rarely extend to >1 MeV.

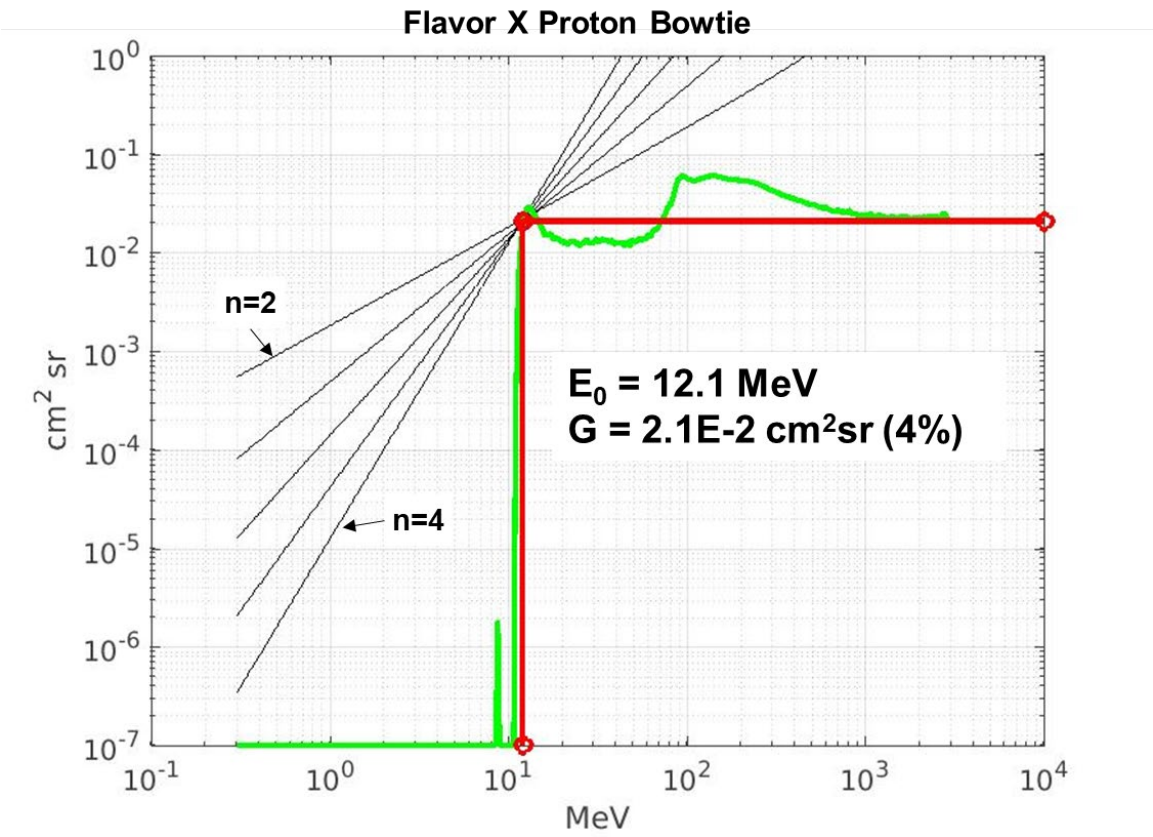

Figure 4. Bowtie analysis for the proton response of flavor X, in the same format as Figure 2.

Figures 5 and 6 summarize the bowtie analysis for all dosimeter flavors for electrons and protons, respectively. Figure 5 shows that, as designed, the electron response in flavor W is suppressed. Figure 6 shows that, as designed, the proton response of flavor W is similar to that of flavor X, allowing flavor W to serve as a proton-only sensor, which can be used to extract the electron-only flux from flavor X, as the two have qualitatively similar proton responses. Flavor Z has a two-step response because its direct access to space (after an 18 μm Al foil) is through a narrow vent hole 14 mil in diameter: low-energy particles can enter only through that hole, while high-energy particles enter from a larger field of view by penetrating the 20 mil Al spacecraft faceplate around the vent hole. The imposition of the power-law tail above >1 MeV for the flavor Z bowtie analysis de-emphasizes these penetrating particles. Under some circumstances, the other dosimeters can be used to determine whether the penetrating particles are present at levels high enough to contribute significantly to the Z dosimeter response, thereby artificially elevating the inferred flux at its bowtie E_0. Likewise, the U, V, and W dosimeters can be used to infer whether there are protons present that could contribute to inferred electron fluxes from the X and Z dosimeters.

In the figures, the horizontal extent of the deviations between the idealized integral channels and the full simulated response function gives a sense of how much spectral structure must be present in order for fluxes derived via the bowtie analysis to become significantly inaccurate. However, for typical conditions, with smooth spectra falling approximately within the ranges of power law and exponential shapes chosen for each dosimeter, the observed count rate can be converted to flux simply by dividing by G.

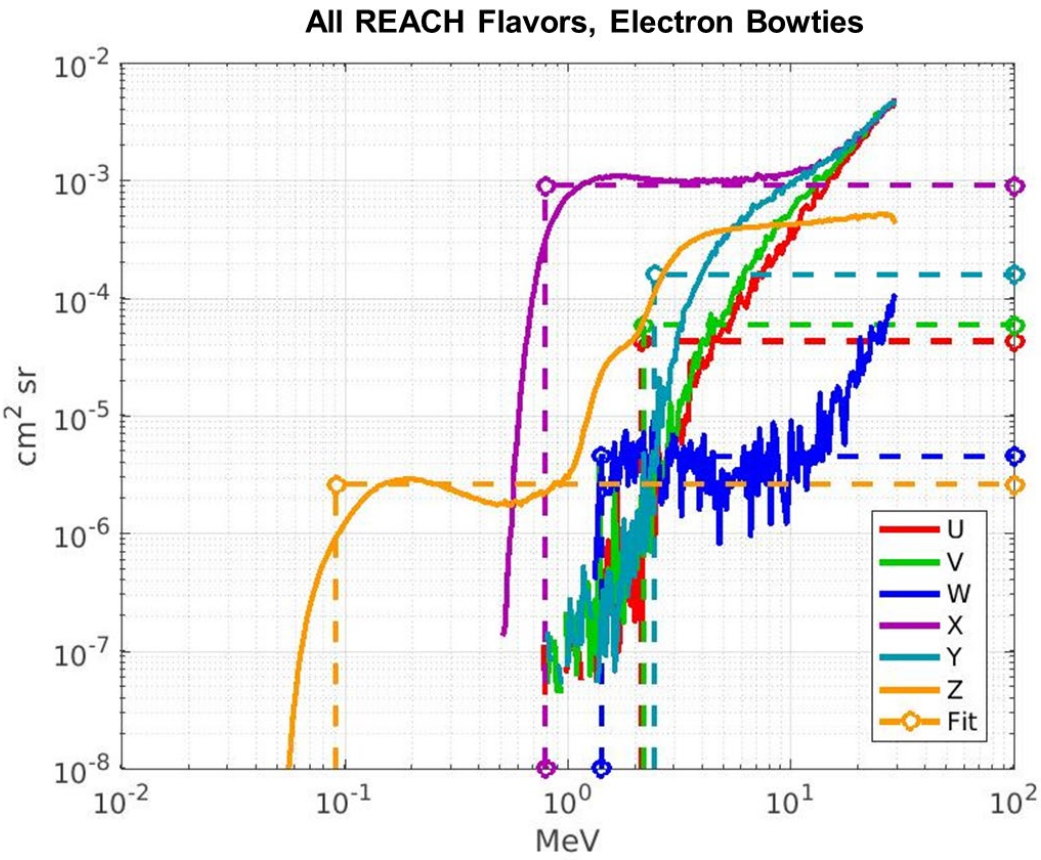

Figure 5. A summary of electron response bowtie analysis results for all six dosimeter flavors. Solid curves provide the response function *R(E)*, while dashed curves provide the fit results for E_0,G.

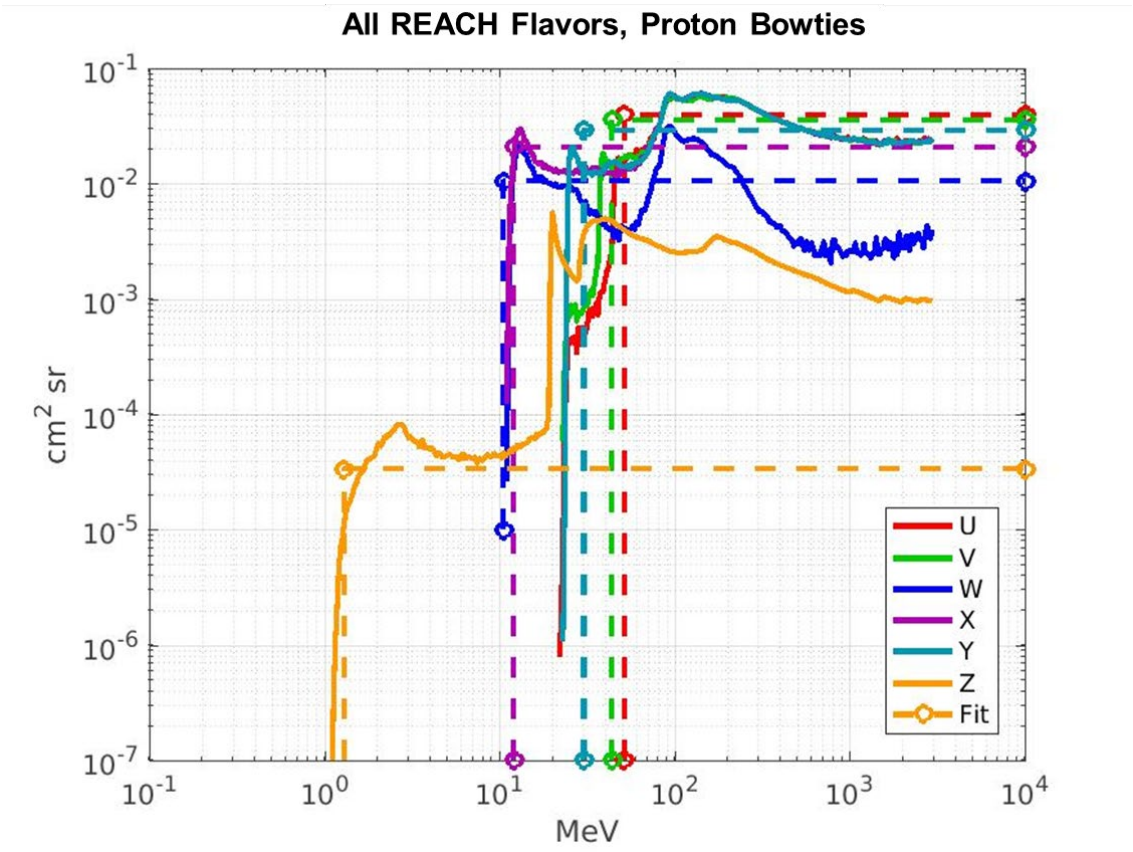

Figure 6. A summary of proton response bowtie analysis results for all six dosimeter flavors. Solid curves provide the response function *R(E)*, while dashed curves provide the fit results for E_0, G.

Table 5 lists the numerical results of the bowtie analysis. The uncertainty in G is derived from the standard deviation of $\ln G$ over the various spectra used in this analysis at the knot in the bowtie. Comparing to Figure 5, we note that when the response function is not sharp near the turn-on or when the response continues to rise after the turn-on, the uncertainty in the flux conversion factors (G) tends to be larger. This uncertainty can be artificially reduced by using only steeply falling spectra, which is why bowtie analysis must always be performed and interpreted carefully.

We have added gray shading to the electron results for flavors U, V, and Y to indicate that, because they do not have any sharp threshold, the bowtie approximation of those sensors to an ideal integral electron channel is highly uncertain. The quantity G is used to convert a count (#/s) rate to an isotropic integral flux (#/cm^2/sr/s). We have also supplied a dose-to-flux conversion factor G^* that can be used to convert a dose rate (rads/s) to an integral flux. G^* is simply G multiplied by the flavor-specific rads/count value from Table 3, noting that we have converted from μrads to rads.

Table 5. Bowtie Results for REACH Dosimeters

Flavor	Electrons				Protons			
	E_0 (MeV)	$G^{(2)}$ (cm^2sr)	$G^{*(3)}$ (cm^2sr rad)	G error[4] (%)	E_0 (MeV)	$G^{(2)}$ (cm^2sr)	$G^{*(3)}$ (cm^2sr rad)	G error[4] (%)
U[1]	2.15	4.3E-5	6.7E-10	110	51.5	4.0E-2	6.2E-7	1
V[1]	2.20	5.9E-5	9.2E-10	103	43.9	3.6E-2	5.6E-7	2
W	1.43	4.5E-6	9.3E-11	7	10.5	1.1E-2	2.2E-7	<1
X	0.798	9.1E-4	1.4E-8	7	12.1	2.1E-2	3.3E-7	4
Y[1]	2.47	1.6E-4	2.5E-9	77	30.3	2.9E-2	4.6E-7	4
Z	0.0916	2.6E-6	7.3E-10	20	1.29	3.3E-5	9.4E-9	9

[1] The approximation to an ideal integral electron channel has large uncertainties for these channels due to the absence of a sharp turn-on in the response function.

[2] Factor for converting dosimeter counts per second to flux.

[3] Factor for converting dosimeter rads per second to flux.

[4] Conversion factor errors are percentages that apply to both G and G^*

4. Summary and Discussion

4.1 Results of Bowtie Analysis

We have performed a bowtie analysis to obtain proton and electron equivalent energy thresholds and flux conversion factors for the six dosimeter flavors carried on the REACH pods. These factors consolidate the full 3-D response obtained from a Geant4 simulation into terms suitable for routine conversion from sensor count rates and dose rates to particle number flux.

The bowtie analysis produces an energy threshold E_0 and a flux conversion factor G, such that the isotropic integral number flux above E_0 can estimated from the dose count rate r according to:

$$j_>(E_0) = \frac{r}{G}$$

with units #/cm^2/sr/s. It is also sometimes useful to compute an omnidirectional number flux $J_>(E_0)$ with units #/cm^2/s, and this would be:

$$J_>(E_0) = 4\pi j_>(E_0) = \frac{4\pi r}{G}$$

The values in Table 5 can be used to evaluate either of these equations to obtain proton or electron number flux estimates from individual REACH dosimeter dose count rates. We also provide G^*, which allows for conversion of dose rates into integral particle flux.

Bowtie analysis provides a convenient way to convert a single channel observation into a particle flux without using other observations or models. However, it has important caveats that apply to dosimeters and to more sophisticated spectrometers: the actual energy response of the sensor does not actually match the idealized integral (or differential) channel response, the angular distribution may not be isotropic over the field of view of the sensor, or the spectral shape may not fall within or sufficiently close to the family of curves used in the bowtie analysis. For many applications, these caveats can be tolerated, and often they can be mitigated by using multiple channels together as checks on each other.

As part of the development of the flux conversion factors, we also produced 3-D (energy-angle-angle) responses for the six dosimeter flavors[1]. These can be integrated over angles to obtain isotropic energy response functions *R(E)*[2]. The energy response functions can be used in 1-D energy spectral inversions, combining multiple dosimeters. The 3-D response curves can be used in data assimilation. Both can be used in data-model comparisons.

4.2 Using These Results

Regardless of whether the source of the particle data is a dosimeter or a more sophisticated spectrometer, fluxes computed from bowtie analyses should not be used in 3-D data assimilation or spectral inversion. Doing so deprives the data assimilative model or spectral inversion of the opportunity to account for, or even exploit, the non-ideal energy and angular response of the sensor. Instead, data

[1] Aerospace employees can access this information in AeroLink at Engineering and Technology Group\Organizations\Physical Sciences Laboratories\Organizations\Space Science Applications\Space Sciences Dept\REACH\Response or https://aerolink.aero.org/cs/llisapi.dll/open/49899912. For people outside of Aerospace, please contact the Aerospace library at 310-336-6736.

[2] This information is also archived in AeroLink. For people outside of Aerospace, please contact the Aerospace library at 310-336-6736.

assimilation should use the 3-D (energy-angle-angle) responses or, if sensor orientation is unknown, the isotropic *R(E)* response function. This is a basic data assimilation technique (e.g., [1]): use the model output to estimate the sensor output, not the other way around. The same applies to all types of data-model comparisons: the model output can be convolved with the 3-D sensor response to estimate the sensor count rate, and the model's skill should be measured against that estimated count rate. This approach avoids dependence on the assumptions of the bowtie analysis, which are unnecessary (and potentially contradictory) when the model is available to provide a full energy-angle distribution of the particles at the location of the sensor.

5. Bibliography

[1] Kalnay, E., Atmospheric Modeling, Data Assimilation and Predictability, Cambridge U. Press, Cambridge, UK, 2003.

[2] Looper, M. D., *Adjoint Monte Carlo Simulations and Improved Sector Shielding Calculations with Geant4*, Aerospace Report Number ATR-2018-00052, The Aerospace Corporation, El Segundo, CA, January 2018.

[3] Looper, M. D., *Comparison of Modeling Techniques for Radiation Dose in a Realistic Geometry*, Aerospace Report Number ATR-2018-00953, The Aerospace Corporation, El Segundo, CA, January 2018.

[4] Looper, M. D., *Proton and Electron Response of the REACH Microdosimeters: Geant4 Simulations*, Aerospace Report Number TOR-2018-02915, The Aerospace Corporation, El Segundo, CA, 2019, in review.

[5] Mazur, J. E.; W. R. Crain; M. D. Looper; D. J. Mabry; J. B. Blake; A. W. Case; M. J. Golightly; J. C. Kasper; and H. E. Spence (2011), New measurements of total ionizing dose in the lunar environment, *Space Weather, 9*, S07002, doi:10.1029/2010SW000641.

[6] Mazur, J. E. et al. (2013), The Relativistic Proton Spectrometer (RPS) for the Radiation Belt Storm Probes Mission, *Space Sci. Rev. 179*(1-4), 221-261, doi:10.1007/s11214-012-9926-9.

[7] O'Brien, T. P.; J. E. Mazur; T. B. Guild; and M. D. Looper (2015), Using Polar-orbiting Environmental Satellite data to specify the radiation environment up to 1200 km altitude, *Space Weather, 13*, doi:10.1002/2015SW001166.

[8] O'Brien, T. P.; J. B. Blake; and J. W. Gangestad (2016), *AeroCube-6 Dosimeter Data README (V3.0)*, Aerospace Report Number TOR-2016-01155, The Aerospace Corporation, El Segundo, CA, March 2016.

[9] O'Brien, T. P.; M. D. Looper; and J. B. Blake, *AeroCube-6 Dosimeter Equivalent Energy Thresholds and Flux Conversion Factors*, Aerospace Report Number TOR-2017-02598, The Aerospace Corporation, El Segundo, CA, 2019, in review

[10] Spence, H. E. et al. (2013), Science goals and overview of the Radiation Belt Storm Probes (RBSP) Energetic Particle, Composition, and Thermal Plasma (ECT) suite on NASA's Van Allen Probes mission, *Space Sci. Rev., 179*(1–4), 311–336, doi:10.1007/s11214-013-0007-5.

AEROSPACE REPORT NO.
TOR-2019-02016

REACH Dosimeter Equivalent Energy Thresholds and Flux Conversion Factors

Approved Electronically by:

James L. Roeder, DIRECTOR
SPACE SCIENCES DEPARTMENT
SPACE SCIENCE APPLICATIONS LABORATORY

Cognizant Program Manager Approval:

Stephen J. Harrington, SYSTEMS DIRECTOR
GROUND SYSTEMS
ENVIRONMENTAL MONITORING
SPACE SYSTEMS GROUP

Aerospace Corporate Officer Approval:

Malina M. Hills, SR VP SPACE SYS
SPACE SYSTEMS GROUP

Content Concurrence Provided Electronically by:

T Paul O'Brien, SCIENTIST SR
MAGNETOSPHERIC & HELIOSPHERIC SCIENCES
SPACE SCIENCES DEPARTMENT

SY0440

AEROSPACE REPORT NO.
TOR-2019-02016

REACH Dosimeter Equivalent Energy Thresholds and Flux Conversion Factors

Technical Peer Review Performed by:

Jeffery M. Cox, PROJECT ENGR SR
SBIRS FOLLOW-ON
ADVANCED PROGRAMS
SPACE SYSTEMS GROUP

SY0440